Fluctuation and Edge-Current Sustainment in a Reversed-Field Pinch

H. Ji,[a] H. Toyama, A. Fujisawa,[a] S. Shinohara, and K. Miyamoto

Department of Physics, Faculty of Science, University of Tokyo, Bunkyo-ku, Tokyo 113, Japan

(Received 14 February 1992)

The simple Ohm's law $\eta j_\parallel = E_\parallel$ is not satisfied in the $a/2 \lesssim r \le a$ region of the REPUTE-1 reversed-field-pinch plasma. Fluctuation-induced electric fields, such as $\langle \tilde{v} \times \tilde{B} \rangle$, are not sufficient to account for $\eta j_\parallel - E_\parallel$ at the edge. Current diffusion due to magnetic fluctuations, carried by fast electrons rather than bulk cold electrons, sustains the edge parallel equilibrium current.

The field-reversal phenomenon, i.e., that the toroidal field reverses its direction at plasma edge in a reversed-field pinch (RFP), has attracted much theoretical and experimental interest constantly since its first observation in the 1960s. Taylor's relaxed-state theory [1] has successfully described the field-reversal configuration as a state of minimum energy, but did not give a physical picture of the relaxation process. Many efforts have been made in order to clarify the governing physical mechanism, especially to explain the sustainment phase of RFPs, in which the reversed field is continuously generated against classical resistive diffusion. Various theoretical models proposed so far can be classified into two broad classes: stochastic field models and MHD turbulent dynamo models. The standard former model is the so-called kinetic dynamo theory (KDT) [2,3], in which the RFP configuration is sustained by radial diffusion of the parallel current due to the stochastic field. The fast electrons, observed recently in the edge [4] or even in the core [5] plasma, are considered as experimental evidence [6] for KDT. Besides this model, there are two models related to the stochastic field; one is the tangled discharge model (TDM), and the other is the resistive evolution model. But recent investigations [7,8] showed that the former is not appropriate for the present RFP, and the latter is closely related to KDT.

The original MHD turbulent dynamo model [9], which is based on an analogy with the geomagnetic dynamo theory, has been developed by a large number of authors [10] (most of them used numerical simulation), but all versions have the same essence, i.e., the assumption of an additional electric field induced by fluctuations in the mean Ohm's law along the mean magnetic field:

$$E_\parallel + \langle \tilde{v} \times \tilde{B} \rangle_\parallel = \eta j_\parallel , \qquad (1)$$

where $E_\parallel$ is the externally applied inductive parallel electric field, η the electric resistivity, $j_\parallel$ the parallel current, and $\tilde{v}$ and $\tilde{B}$ the fluctuating fluid velocity and magnetic field, respectively. However, the fluctuation-induced electric field $\langle \tilde{v} \times \tilde{B} \rangle_\parallel$ has never been measured in the laboratory; thus the dynamo hypothesis has not yet been confirmed. In this Letter, we report the results of fluctuation measurements focusing on the fluctuation-induced electric field in the $a/2 \lesssim r \le a$ region of the REPUTE-1

[11] RFP plasma, which has a major radius of $R = 82$ cm and a minor radius of $a = 22$ cm. All terms in Eq. (1) including $\langle \tilde{v} \times \tilde{B} \rangle_\parallel$ are examined experimentally. Some discussion about other possible terms in the parallel Ohm's law, including that originating from current diffusion, is also given.

Because the diagnostics used here have been already described in detail in other published works [12,13], we give only a brief summary. A triple-probe technique was developed [12] in order to meet the need to measure the mean ($f < 5$ kHz, denoted by overbars) and fluctuation parts ($5 \le f \le 70$ kHz, denoted by tildes) of the plasma density n, electron temperature T_e, and space potential ϕ_s (measured with respect to the wall potential) simultaneously in a fluctuating plasma. The fast electrons also may have effects on the probe measurements, but they are not expected to give significant perturbations to our measurements [12,13].

A complex probe [12], which consists of a triple probe (measuring n and T_e), a three-component magnetic probe (measuring B_t, B_p, and B_r), and three pairs of double probes (measuring electric field E_t, E_p, and E_r), has been constructed in order to determine correlations between the fluctuations. All of them are placed within a space of 10 mm × 10 mm × 15 mm. Here, we must note that the electric field $\tilde{E}' \equiv -\nabla \tilde{\phi}_f$ (ϕ_f is the floating potential) measured by a double probe is different from $\tilde{E} \equiv -\nabla \tilde{\phi}_s$, due to a finite $\tilde{T}_e$ as a result of the relation of $\tilde{E}' = \tilde{E} + c \nabla \tilde{T}_e$, where c is a constant $\simeq 2.1$ [12] in our case.

In order to avoid damages to the inserted probes, discharges were carried out at the relatively low plasma current ($I_p \sim 110$ kA). All measured quantities presented here are taken from the time interval of 0.2 ms around the current flattop. The loop voltage V_l, the reversal ratio F, the pinch parameter Θ, and the chord-averaged density $\bar{n}_e$ are $V_l \sim 220$ V, $F \sim -0.4$, $\Theta \sim 2.0$, and $\bar{n}_e \sim 4.4 \times 10^{19}$ m^{-3}, respectively.

Radial profiles of the mean values of $\bar{B}_t$ and $\bar{B}_p$ are shown in Fig. 1(a), where the error bars indicate the shot-by-shot variation. Polynomial functions are fitted to $\bar{B}_t$ and $\bar{B}_p$ profiles under the constraints that the toroidal and poloidal currents, $\bar{j}_t = (1/\mu_0 r) \partial(r\bar{B}_p)/\partial r$ and $\bar{j}_p = -(1/\mu_0) \partial \bar{B}_t/\partial r$ fall to zero at $r = a$. Figure 1(b) shows the profiles of $\bar{j}_t$, $\bar{j}_p$, and $j_\parallel \equiv \bar{j} \cdot \bar{B}/B$ (B is the total
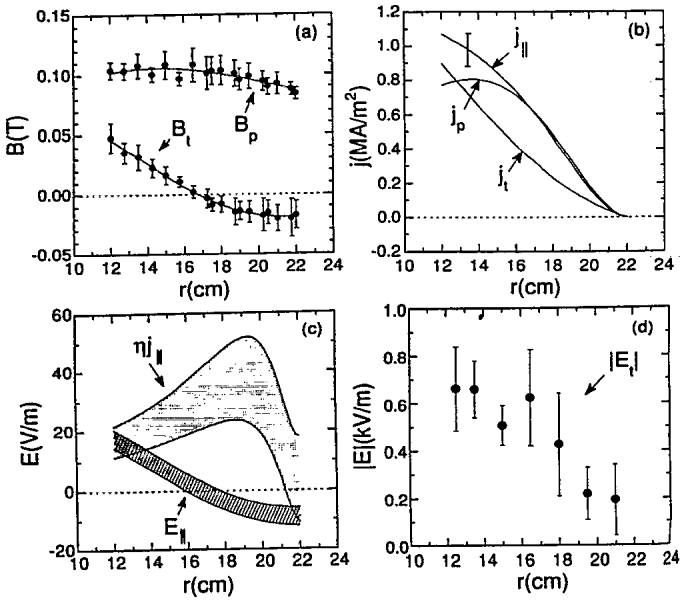
FIG. 1. Radial profiles of (a) $\bar{B}_t$ and $\bar{B}_p$ [fitting curves by polynomial functions under the constraints of $\bar{j}_t(a) = \bar{j}_p(a) = 0$ are also shown]; (b) $\bar{j}_t$, $\bar{j}_p$, and $j_\parallel \equiv \bar{j} \cdot \bar{B}/B$; (c) resistive electric field $\eta j_\parallel$ and externally applied inductive electric field $E_\parallel$; and (d) fluctuation level of $\tilde{E}_t'$.

field), where the error bar comes from the fitting procedures due to error propagation. A significant perpendicular current can be obtained in the same way, implying that there might be a deep gradient in the pressure profile at the edge. Figure 1(c) shows the radial profile of $\eta j_\parallel$, where the Spitzer resistivity η is obtained from the

measured profile [13] of $\bar{T}_e$ assuming $Z_{\text{eff}} = 1.5$. The parallel component of the externally applied toroidal inductive electric field $E_\parallel$, given by $(V_l/2\pi R)\bar{B}_t/B$ in the steady state, is also shown. The simple Ohm's law $\eta j_\parallel = E_\parallel$ is not satisfied. The difference between $\eta j_\parallel$ and $E_\parallel$ must be accounted for by the fluctuation-induced electric field $\langle \tilde{v} \times \tilde{B} \rangle_\parallel$ according to the MHD dynamo model in Eq. (1). Note that the assumption of classical resistivity and low Z_{eff} gives the minimum for this difference.

Radial profiles of the magnetic fluctuation level had been measured [13]. At $r \sim a$, $|\tilde{B}_t|/B \sim 2\%$ is about twice the value of $|\tilde{B}_p|/B \cong |\tilde{B}_r|/B \sim 1\%$, but at $r \sim a/2$, $|\tilde{B}_r|/B \sim 3\%$ is about twice that of $|\tilde{B}_t|/B \cong |\tilde{B}_p|/B \sim 1.5\%$. As the radius decreases to $r \sim a/2$, $|\tilde{E}_t|$ [shown in Fig. 1(d)], $|\tilde{E}_p|$, and $|\tilde{E}_r|$ measured by the complex probe increase to ~ 0.7, ~ 0.5, and ~ 0.9 kV/m, respectively.

Although a MHD dynamo model usually ignores effects arising from two-fluid treatments, we start from the generalized Ohm's law [14], i.e., $\mathbf{E} + \mathbf{v} \times \mathbf{B} - \nabla P_i/(en) = \eta \mathbf{j}$, where $P_i = nT_i$ is the ion pressure. Other terms in the original generalized Ohm's law can be shown to be negligible in our case. Then the perpendicular velocity fluctuation becomes

$$\tilde{v}_\perp = [\tilde{\mathbf{E}} - \nabla \tilde{P}_i/(en) - \tilde{\eta}\tilde{j} + \tilde{v} \times \tilde{B}] \times \bar{B}/B^2. \quad (2)$$

From the fact that $|\tilde{B}|/B \lesssim 3\%$, $|\tilde{T}_e|/\bar{T}_e \sim 25\%$, $|\tilde{j}|/j \sim 30\%$ [15], and $\bar{v} \sim E_r/B \sim [\phi_s(a/2)/(a/2)]/B \sim 2$ km/s [13], it is easy to find that the third and fourth terms are negligibly small compared to the first term on the right-hand side (rhs) of Eq. (2). Because $\langle \tilde{v} \times \tilde{B} \rangle_\parallel = \langle \tilde{v}_\perp \times \tilde{B}_\perp \rangle_\parallel = \langle [\tilde{\mathbf{E}}_\perp + \nabla_\perp \tilde{P}_i/(en)] \cdot \tilde{B}_\perp \rangle/B$, the parallel mean Ohm's law becomes

$$\eta j_\parallel - E_\parallel = \langle \tilde{v} \times \tilde{B} \rangle_\parallel + \langle \tilde{n} \nabla_\parallel \tilde{P}_i \rangle/(e\bar{n}^2) - \langle \tilde{\eta}\tilde{j}_\parallel \rangle = \text{Re}\{\langle [\tilde{\mathbf{E}}_\perp' - i c k_\perp \tilde{T}_e - \nabla_\perp \tilde{P}_i/(en)] \cdot \tilde{B}_\perp \rangle/B + i k_\parallel \langle \tilde{n} \tilde{T}_i \rangle/\bar{n}\}, \quad (3)$$

where $\langle \tilde{\eta}\tilde{j} \rangle \ll \eta j$. Note that

$$\nabla_\perp \tilde{P}_i/(en) = (i k_\perp - L_n^{-1} \mathbf{e}_r)\tilde{T}_i + (\bar{T}_i/\bar{n})(i k_\perp + L_n^{-1} \mathbf{e}_r)\tilde{n},$$

where $\mathbf{e}_r$ is the radial unit vector and $L_n \equiv -\bar{n}(\partial \bar{n}/\partial r)^{-1}$. Here we ignored the $\partial/\partial r$ contribution in $\nabla_\perp$, because the fluctuations are well correlated and almost in phase over at least half a radius, especially at the low frequency. The inductive part of $\tilde{\mathbf{E}}_\perp$ can be estimated simply by $(\omega/k_\parallel)|\tilde{B}_r|$ where $f \sim 15$ kHz and $k_\parallel \sim 1/a$, which is one order smaller than the electrostatic part. Thus the fluctuation-induced electric fields depend on correlations between electrostatic ($\tilde{\mathbf{E}}$, $\tilde{n}$, $\tilde{T}_e$, and $\tilde{T}_i$) and magnetic ($\tilde{\mathbf{B}}$) fluctuations

It is found that the magnetic fluctuations show an entirely different behavior from the electrostatic ones, which are well correlated with each other [13]. For example, the squared coherences γ^2 between $\tilde{T}_e$ and $\tilde{E}_t'$, $\tilde{T}_e$ and $\tilde{B}_t$, and $\tilde{B}_t$ and $\tilde{E}_t'$ are shown in Fig. 2. Coherences are usually not less than ~ 0.5 in most of the frequency range between the electrostatic fluctuations, but below ~ 0.2 between the electrostatic ones and magnetic ones, consistent

with MST experiments [16]. Hence there are almost no correlations between these two types of fluctuations. Indeed, the normalized correlation coefficients $C_{\alpha,\beta} \equiv \langle \tilde{\alpha}\tilde{\beta} \rangle/|\tilde{\alpha}||\tilde{\beta}| \equiv \int \gamma^2 \cos\theta \, d\omega$ and the phase-shifted correlation coefficients $C_{\alpha,\beta}' \equiv i\langle \tilde{\alpha}\tilde{\beta} \rangle/|\tilde{\alpha}||\tilde{\beta}| \equiv \int \gamma^2 \cos(\theta + \pi/2) d\omega$
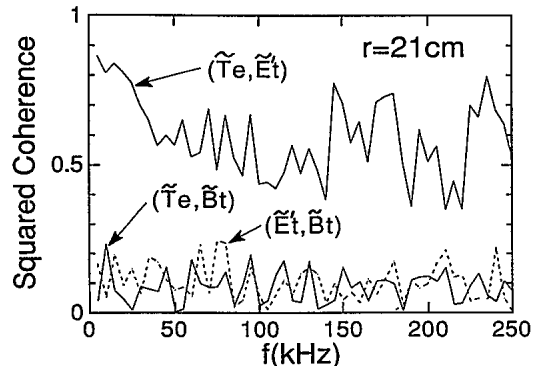

FIG. 2. Squared coherence between $\tilde{T}_e$ and $\tilde{E}_t'$, $\tilde{T}_e$ and $\tilde{B}_t$, and $\tilde{B}_t$ and $\tilde{E}_t'$ as functions of frequency.
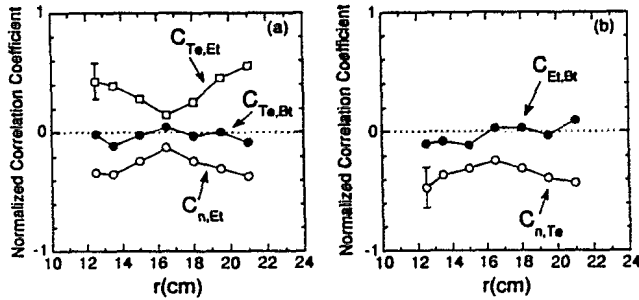
FIG. 3. Radial profiles of normalized correlation coefficients: (a) C_{T_e,B_t}, $C_{T_e,E_t'}$, and $C_{n,E_t'}$; (b) C_{E_t',B_t} and C_{n,T_e}.

are ~ 0 across the outer half radius (here $a = E_t', E_p'$, E_r', n, T_e; $\beta = B_t, B_p, B_r$). As an example, profiles of C_{T_e,B_t} and C_{E_t',B_t} are shown in Figs. 3(a) and 3(b), respectively. Spatial spread of the complex probe is not expected to induce these decorrelations, because the same types (electrostatic or magnetic) of fluctuations are still well correlated with each other, even when they are measured over a longer distance. Electrostatic fluctuations $\tilde{n}$, $\tilde{T}_e$, and $\tilde{E}'$ show clear positive or negative correlations [13], as also shown in Fig. 3. In Fig. 4, the region bounded by lines with open circles shows the measured value of the first term in Eq. (3) including the correlations, and the shaded region shows $\eta j_\parallel - E_\parallel$ calculated from Fig. 2.

Spectra for the electrostatic fluctuations are broader [16] than those for the magnetic ones, with widths of $\Delta m \sim 3$ and $\Delta n \sim 70$. Here we use $|k_\parallel| \sim \Delta m/2a \sim 1.5/a$ and $|k_\perp| \sim \Delta n/2R \sim 35/R$ as typical values. The ion temperature T_i at the edge is unmeasured, but an assumption of $T_i \sim 2T_e$ would be reasonable, because $T_i(0) \sim 100$ eV
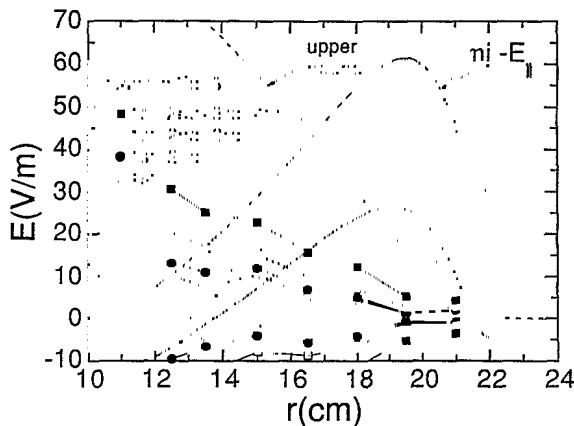

FIG. 4. Comparisons between radial profiles of $\eta j_\parallel - E_\parallel$ (shown as the shaded region) and fluctuation-induced electric fields (shown as regions between lines with the *same* symbols). Values of the first through the fourth terms on the rhs of Eq. (3) are indicated by O, ●, □, and ■, respectively. The dashed line shows the upper bound of fluctuation-induced electric fields assuming complete correlations.

at the center, measured by the Doppler broadening of the O V line, is about twice the value of $T_e(0) \sim 50$ eV, measured by a Thomson scattering system. Since $L_n \sim 0.1$ m in the REPUTE-1 RFP, the second through the fourth terms on the rhs of Eq. (3) can be evaluated assuming $|C_{T_i,n}| = |C_{T_i,B}| = 1$. These values are also shown in Fig. 4. We find that the sum of all possible fluctuation-induced electric fields cannot sustain the parallel equilibrium current in the region where B_t is reversed ($r \gtrsim 17$ cm). Even the upper bound values of total fluctuation-induced electric field (when all fluctuations are completely correlated), shown as a dashed line in Fig. 4, still cannot account for $\eta j_\parallel - E_\parallel$ near the edge.

Next we examine another possible mechanism for sustaining the edge parallel current, i.e., that there exists an outward flux of parallel electron current (or momentum) $\Gamma_{\text{tot}}(r)$ satisfying $\eta j_\parallel - E_\parallel + (1/r)\partial(r\Gamma_{\text{tot}})/\partial r = 0$ as in kinetic dynamo theory [2]. We have

$$\Gamma_{\text{tot}}(r) = (a/r)\Gamma_{\text{tot}}(a) + (1/r)\int_r^a (\eta j_\parallel - E_\parallel) r \, dr. \quad (4)$$

Here $\Gamma_{\text{tot}}(a)$ is the electron-current (momentum) loss to the wall, which has been used to explain the anomalous resistivity observed in RFPs [3]. From the electron drift kinetic equation, radial fluxes of parallel current due to electrostatic and magnetic fluctuations are given by [17]

$$\Gamma_E = \frac{m_e j_\parallel}{e^2 n}\left\langle \frac{\tilde{\mathbf{E}} \times \overline{\mathbf{B}}}{B^2} \cdot \mathbf{e}_r \frac{\tilde{j}_\parallel}{j_\parallel} \right\rangle, \quad \Gamma_B = \frac{T_e}{e}\left\langle \frac{|\tilde{B}_r|}{B} \frac{\tilde{p}_{e\parallel}}{p_{e\parallel}} \right\rangle,$$

respectively. Another expression for the radial flux of parallel current is $\Gamma_{\text{st}} = -\lambda_{\text{st}}(1/r)\partial(rj_\parallel)/\partial r$, where λ_{st} is the current viscosity [18]. The current diffusion due to stochastic field [19] is related to electron heat transport [20] by $\lambda_{\text{st}} = -\chi_{\text{st}} m_e/(e^2 n)$, where the electron thermal diffusivity χ_{st} is $(8/\pi)^{1/2} v_{\text{th}}^e L_\parallel (|\tilde{B}_r|/B)^2$, v_{th}^e is the electron thermal velocity, and $L_\parallel \sim 0.35$ m in our case [13]. Values of Γ_E, Γ_B, and Γ_{st} can be estimated with the use of measured mean quantities and their fluctuation levels, assuming $C_{B_r,p_{e\parallel}} = C_{E,j_\parallel} = 1$ and $p_{e\parallel} = p_e$. However, they all are at least one order smaller than Γ_{tot}. For example, the values at $r = 19$ cm are given in the first column in Table I.

TABLE I. Comparisons between total flux and fluctuation-driven fluxes of electron current at $r = 19$ cm in the cases of bulk cold electrons and fast electrons. Here $\Gamma_{\text{tot}}' \equiv \Gamma_{\text{tot}}(r) - (a/r)\Gamma_{\text{tot}}(a)$. Note that $T_e(0) \sim 50$ eV.

	Bulk cold electrons	Fast electrons	
T_e^F (eV)		50	100
T_e^F/T_e		8.6	17.2
n^F/n		13.1%	9.3%
η^F/η		0.94	0.47
Γ_{tot}' (V)	0.87 ± 0.21	0.58 ± 0.23	0.41 ± 0.16
Γ_E (V)	~ 0.001	~ 0.02	~ 0.03
Γ_B (V)	~ 0.05	~ 0.33	~ 0.66
Γ_{st} (V)	~ 0.01	~ 0.34	~ 0.67

The above estimates are based on the assumption that the current is carried by the bulk cold electrons. However, it has been observed that the current is mainly carried by the fast electrons at the edge [4] and also in the core [5] region. If $j_\parallel$ is carried only by the fast electrons with density $n^F \equiv \alpha n$ and temperature $T_e^F = \beta T_e$, we have $\alpha\sqrt{\beta} = j_\parallel/(env_{th}^e)$, under the assumption of a half-Maxwellian velocity distribution [6]. Relations of $\Gamma_E^F = \Gamma_E \alpha^{-1}$, $\Gamma_B^F = \Gamma_B \beta$, and $\Gamma_{st}^F = \Gamma_{st}\alpha^{-1}\sqrt{\beta}$ can be also easily obtained with the assumption of the same fluctuation levels and correlations. The electric resistivity η^F of the fast electrons is also different from η: $\eta^F/\eta = 3\sqrt{\pi}(2+Z_{\text{eff}})/(4Z_{\text{eff}})\alpha^{-1}\beta^{-3/2}$, where frictional forces due to the bulk cold electrons and ions are included. Note that η^F can be larger than η depending on α and β. We can obtain Γ_{tot}^F by replacing η in Eq. (4) by η^F. Table I lists the estimated values of radial fluxes of parallel current in the two cases of $T_e^F = 50$ eV $[\sim T_e(0)]$ and $T_e^F = 100$ eV $[\sim 2T_e(0)]$ at $r = 19$ cm. It can be seen that Γ_B^F or Γ_{st}^F could account for Γ_{tot}^F while Γ_E^F still does not. This suggests that the magnetic fluctuations may play an important role in sustaining the edge parallel current.

So far studies on stochastic diffusion are all based on prescribed (i.e., not self-consistent) stochastic fields. A recent self-consistent treatment [21] showed that the current diffusion becomes much smaller than the quasilinear result. However, the fast electrons argued for here are not affected by self-consistency constraints, since they are fast enough to decouple from the waves.

In conclusion, electrostatic fluctuations ($\tilde{E}$, $\tilde{n}$, $\tilde{T}_e$) are almost uncorrelated with magnetic ones ($\tilde{B}$) in the $a/2 \lesssim r \leq a$ region of the REPUTE-1 RFP. Fluctuation-induced electric fields, such as $\langle \tilde{v} \times \tilde{B} \rangle$, are experimentally examined for the first time. It is found that these fluctuation-induced electric fields are not sufficient to account for $\eta j_\parallel - E_\parallel$, at least in the B_t-reversed region, not supporting the basic hypothesis of MHD turbulent dynamo models. On the other hand, it appears that current diffusion due to magnetic fluctuations, carried by fast electrons rather than bulk cold electrons, sustains the edge parallel equilibrium current.

At the present stage, it is impossible to affirm one or the other of these two classes of models. But our experimental results reported in this Letter imply that KDT might be more suitable than MHD dynamo models for the description of the actual RFP edge region. For the interior region, it is more difficult to examine these models. Some combination of MHD and kinetic dynamo models may provide a better description. In fact, they are both based on the common assumption of a turbulent state of plasma.

[a]Present address: National Institute for Fusion Science, Nagoya 464-01, Japan.

[1] J. B. Taylor, Phys. Rev. Lett. 33, 1139 (1974).

[2] A. R. Jacobson and R. W. Moses, Phys. Rev. A 29, 3335 (1984).

[3] R. W. Moses, K. F. Schoenberg, and D. A. Baker, Phys. Fluids 31, 3152 (1988).

[4] J. C. Ingraham et al., Phys. Fluids B 2, 143 (1990).

[5] Y. Yagi et al., Plasma Phys. Controlled Fusion 33, 1391 (1991).

[6] K. F. Schoenberg and R. W. Moses, Phys. Fluids B 3, 1467 (1991).

[7] M. G. Rusbridge, Plasma Phys. Controlled Fusion 33, 1381 (1991).

[8] G. Miller, Phys. Fluids B 3, 1182 (1991).

[9] C. G. Gimblett and M. L. Watkins, in Proceedings of the Seventh European Conference on Controlled Fusion and Plasma Physics, Lausanne, 1975 (European Physical Society, Geneva, 1975), Vol. 1, p. 103.

[10] For example, the earliest simulation result is E. J. Caramana, R. A. Nebel, and D. D. Schnack, Phys. Fluids 26, 1305 (1983), and the newest one is Y. L. Ho and G. G. Craddock, Phys. Fluids B 3, 721 (1991).

[11] N. Asakura et al., Nucl. Fusion 29, 893 (1989).

[12] H. Ji et al., Rev. Sci. Instrum. 62, 2326 (1991).

[13] H. Ji et al., Phys. Rev. Lett. 67, 62 (1991).

[14] K. Miyamoto, Plasma Physics for Nuclear Fusion (MIT, Cambridge, MA, 1980), Chap. 6.

[15] T. Oikawa (private communication); in REPUTE-1 Annual Report, 1991 (to be published).

[16] T. D. Rempel et al., Phys. Rev. Lett. 67, 1438 (1991).

[17] S. C. Prager, Plasma Phys. Controlled Fusion 32, 903 (1990).

[18] J. Schmidt and S. Yoshikawa, Phys. Rev. Lett. 26, 753 (1971).

[19] T. H. Stix, Nucl. Fusion 18, 353 (1978).

[20] A. B. Rechester and M. N. Rosenbluth, Phys. Rev. Lett. 40, 38 (1978).

[21] P. W. Terry and P. H. Diamond, Phys. Fluids B 2, 1128 (1990).